

1 **Rubber plant root properties induce contrasting soil aggregate stability**
2 **through cohesive force and reduced land degradation risk in southern China**

3 Waqar Ali¹, Amani Milinga¹, Tao Luo², Mohammad Nauman Khan³, Asad Shah³, Khurram
4 Shehzad⁵, Qiu Yang¹, Huai Yang⁴, Wenxing Long¹, Wenjie Liu^{1*}

5 *¹Center for Eco-Environment Restoration Engineering of Hainan Province, School of Ecology,*
6 *Hainan University, Haikou, 570228, China.*

7 *²CSIRO Agriculture and Food, Private Bag 5, Wembley, WA 6913, Australia.*

8 *³School of Breeding and Multiplication (Sanya Institute of Breeding and Multiplication), Hainan*
9 *University, Haikou, 570228, China*

10 *⁴Institute of Tropical Bamboo, Rattan & Flower, Sanya Research Base, International Center for*
11 *Bamboo and Rattan, Sanya 572000, China*

12 *⁵Hubei Key Laboratory of Soil Environment and Pollution Remediation, College of Resources and*
13 *Environment, Huazhong Agricultural University, Wuhan, 430070, China*

14

15

16 *** Corresponding authors:** Wenjie Liu

17 E-mail: liuwj@hainanu.edu.cn

18 Tel: 86-17733181789

19

20 **Abstract**

21 In southern China, Hainan Island faces land degradation risks due to a combination of soil
22 physical, chemical, and climatic factors. Specifically, soil physical properties like a high
23 proportion of microaggregates (<0.25 mm), chemical properties such as low soil organic matter
24 (SOM) content, and a climatic factor of frequent uneven rainfall. The cohesive force between soil
25 particles, which is influenced by plant root properties and root-derived SOM, is essential for
26 improving soil aggregate stability and mitigating land degradation. However, the mechanisms by
27 which rubber plant root properties and root-derived SOM affect soil aggregate stability through
28 cohesive forces in tropical regions remain unclear. This study evaluated rubber plants of different
29 ages to assess the effects of root properties and root-derived SOM on soil aggregate stability and
30 cohesive forces. Older rubber plants (> 11-years-old) showed greater root diameters (RD) (0.81–
31 0.91 mm), higher root length (RL) densities (1.83–2.70 cm cm⁻³), and increased proportions of fine
32 (0.2–0.5 mm) and medium (0.5–1 mm) roots, leading to higher SOM due to lower lignin and higher
33 cellulose contents. Older plants exhibited higher soil cohesion, with significant correlations among
34 root characteristics, SOM, and cohesive force, whereas the random forest (RF) model identified
35 aggregates (> 0.25 mm), root properties, SOM, and cohesive force as the key factors influencing
36 mean weight diameter (MWD) and geometric mean diameter (GMD). Furthermore, partial least
37 squares-path models (PLS-PM) showed that the RL density (RLD) directly influenced SOM (path
38 coefficient 0.70) and root-free cohesive force (RFCF) (path coefficient 0.30), which subsequently
39 affected the MWD, with additional direct RLD effects on the SOM (path coefficient 0.45) and
40 MWD (path coefficient 0.64) in the surface soil. Cohesive force in rubber plants of different ages
41 increased macroaggregates (> 0.25 mm) and decreased microaggregates (< 0.25 mm), with topsoil
42 average MWD following the order: Control (CK) (0.98 mm) < 5Y_RF (1.26 mm) < MF (1.31 mm)

43 $< 11Y_RF$ (1.36 mm) $< 27Y_RF$ (1.48 mm) $< 20Y_RF$ (1.51 mm). Rubber plant root traits
44 improve soil aggregate stability and mitigate land degradation risk in tropical regions. Rubber plant
45 root traits enhance soil aggregate stability and mitigate land degradation risk in tropical regions,
46 offering practical soil restoration strategies through targeted root trait selection to strengthen soil
47 cohesion, ensure long-term agricultural productivity, and preserve environmental quality,
48 highlighting the need for further research across diverse ecological zones and forest types.

49 **Keywords:** Rubber plant root traits; soil organic matter; cohesive force; aggregate stability; land
50 degradation

51 1. Introduction

52 Land degradation is a serious global issue that increases as a consequence of growing
53 population and climate change, currently impacting $> 75\%$ of land and projected to affect $> 90\%$
54 by 2050 (Perović et al., 2021; Práválie et al., 2021; Thomas et al., 2023). Land degradation in
55 tropical regions, such as Hainan Island, southern China, is driven by unfavorable soil conditions,
56 including a high proportion of microaggregates (<0.25 mm), which reduces soil stability, and low
57 soil organic matter (SOM) content, which weakens soil structure. Land degradation in tropical
58 regions, such as Hainan Island, southern China, is driven by unfavorable soil conditions, including
59 a high proportion of microaggregates (<0.25 mm) often observed in degraded soils due to
60 macroaggregate breakdown which reduces structural stability, water infiltration, and low soil
61 organic matter (SOM) content, which further weakens soil structure. Additionally, the uneven and
62 high frequency of rainfall events during the summer season (May–October), combined with global
63 climate change, further intensifies water erosion and accelerates land degradation (Shao et al.,
64 2024; Zhu et al., 2022). In addition, zonal ferro-alumina lateritic soils (ferralsols) on Hainan Island,
65 classified as having low resilience and sensitivity according to the tropical soil resilience-

66 sensitivity matrix, are particularly prone to soil erosion (Li et al., 2022). Consequently, the current
67 soil erosion area on Hainan Island has increased 4.8-fold compared to that in 2000, according to a
68 third national soil erosion remote-sensing survey (Yu et al., 2016). Soil aggregates are fundamental
69 to soil function, and their stability regulates carbon cycling, nutrient storage, soil fertility,
70 infiltration rate, and resistance to soil degradation (Hok et al., 2021; Rabot et al., 2018; Yudina and
71 Kuzyakov, 2023). Therefore, it is imperative to enhance soil aggregate stability by implementing
72 suitable management practices that protect the integrity of the environment and ensure sustainable
73 agricultural productivity.

74 Natural rubber (*Hevea brasiliensis* *Willd. ex A. Juss*) plantations have recently expanded
75 rapidly across mainland Southeast Asia (Xu et al., 2023; Yang et al., 2024). Rubber plants are
76 recognized for their effectiveness in improving soil aggregate stability through their root properties
77 and in mitigating soil erosion (Kurmi et al., 2020; Sun et al., 2021). Root morphology, particularly
78 traits like fine roots length (FRL), coarse roots length (CRL), root diameter (RD), and root length
79 density (RLD), influences soil structure by enhancing particle binding. Fine roots, with their higher
80 surface area, increase root-soil contact, promoting stronger aggregate formation through
81 entanglement and cohesive force.cohesion Plant roots influence soil aggregate size distribution by
82 promoting FRL, which closely interacts with soil particles, and negatively affecting CRL, which
83 disintegrate into larger particles (Ali et al., 2022; Chen et al., 2021; Kumar et al., 2017). Plant
84 morphological root traits, such as RD and RLD, and their chemical composition, including lignin
85 and cellulose content, have been shown to alter carbon deposits in soil pools and their sequestration
86 (Poirier et al., 2018b; Rossi et al., 2020). Nevertheless, several studies have suggested that the
87 interaction between soil particles and plant root-derived SOM is limited, which significantly
88 affects soil particle stability through cohesive forces, particularly after root decomposition (Ali et

89 al., 2022; Chen et al., 2017). Variations in soil particles and root-derived SOM further adjust soil
90 cohesion.

91 Soil cohesive forces, derived from SOM and the morphological and chemical properties of
92 plant roots (Wang et al., 2018a; Wang et al., 2020), effectively stabilize sloped soils by enhancing
93 soil-particle interactions, promoting flocculation, and minimizing soil erosion, thereby controlling
94 soil and water runoff (Smith et al., 2021; Wang et al., 2018a). Among these factors, SOM plays a
95 complex role and is generally beneficial for promoting particle flocculation. However, an excess
96 charge on SOM, combined with the negative charges of soil particles, can also lead to the
97 dispersion of aggregates (He et al., 2021; Melo et al., 2021). The addition of plants and their roots
98 allows for additional soil organic carbon (SOC) accumulation in the soil (Rossi et al., 2020). Roots
99 can also bind soil particles via cohesive forces, thus increasing aggregate stability (Forster et al.,
100 2022; Poirier et al., 2018a; Wang et al., 2020). Dominant root traits influence soil particles through
101 cohesive forces, and their subsequent effects on soil aggregate stability remain unknown.

102 So far, few studies have investigated the impact of rubber plant roots on soil aggregation
103 in the tropical region of Hainan Island (Sun et al., 2021; Zou et al., 2021), and there is a complete
104 lack of research regarding the mechanisms related to rubber plant root morphological and chemical
105 properties, root-derived SOM, and cohesive forces in aggregate formation. We hypothesized that
106 rubber plantations of different stand ages would promote soil cohesive forces through root
107 properties and SOM among soil particles, ultimately improving aggregate stability. This study
108 aimed to: 1) investigate the impact of stand-age rubber plant root traits and root-derived SOM on
109 aggregate properties, and 2) explore the interconnections between root morphological and
110 chemical characteristics, SOM, cohesive forces, and soil aggregate stability. The findings of this
111 research will contribute to better management practices in the tropical regions of Hainan Island,

112 helping to mitigate land degradation issues by enhancing aggregate stability and overall
113 environmental quality.

114 **2. Materials and methods**

115 *2.1. Experimental site overview*

116 The study was conducted on Hainan Island in Danzhou ($19^{\circ}4'3''$ – $19^{\circ}12'42''$ N, and $109^{\circ}47'6''$ – $110^{\circ}1'2''$ E, 182–255 m above sea level). In the study area, the annual averages for temperature,
117 precipitation, and solar radiation are 23.5°C , 1831 mm, and $4579 \text{ MJ}\cdot\text{m}^{-2}\cdot\text{yr}^{-1}$, respectively.
118 November–April of the following year is the dry season, whereas May–October is the rainy season.
119 Rubber (*Hevea brasiliensis*) and areca (*Areca catechu* L.) are the two primary commercial crops
120 in the experimental region. Prior to rubber plantation, the land was covered by tropical rainforest.
121 According to the USA Soil Taxonomy System, the soil is classified as a laterite ferralsol (Schad,
122 2023). The soil in the rubber plantation was composed of 43.71% sand, 8.28% silt, and 48.01%
123 clay. The basic physical and chemical characteristics of the samples are listed in Table. 1.

125 *2.2. Experimental design*

126 Rubber plantations with four different stand ages were selected from the field. The
127 treatments included five-year-old rubber forests (5Y_RF), with 2018 rubber trees (clone PR-107)
128 planted at the recommended density ($3 \times 7 \text{ m}$, $480 \text{ plants}\cdot\text{ha}^{-1}$) and crown density 30 %; 11-year-
129 old rubber forests (11Y_RF), with 2012 rubber trees (clone PR-107) planted at the recommended
130 density ($3 \times 7 \text{ m}$, $431 \text{ plants}\cdot\text{ha}^{-1}$) and crown density 90 %; 20-year-old rubber forests (20Y_RF),
131 with 2003 rubber trees (clone PR-107) planted at the recommended density ($3 \times 7 \text{ m}$, 346
132 $\text{plants}\cdot\text{ha}^{-1}$) and crown density 90 %; 27-year-old rubber forests (27Y_RF), with 1996 rubber trees
133 (clone PR-107) planted at the recommended density ($3 \times 7 \text{ m}$, $300 \text{ plants}\cdot\text{ha}^{-1}$) and crown density
134 90 %; and mixed forest (MF) and control (no forest plants) (CK). The MF treatment represents a

135 mixed forest system consisting of cinnamon (*Cinnamomum verum*) trees (planted in 2014)
136 intercropped with 20-year-old rubber (*Hevea brasiliensis*) trees. This treatment was included to
137 assess the potential benefits of mixed-species plantations on soil aggregation and stability
138 compared to monoculture rubber plantations. We established a randomized complete block design
139 with three replicates. We selected 18 plots (30 × 30 m) separated by a transitional zone. Rubber
140 plants with different stand ages were selected based on similar topographies (slope and gradient)
141 and management practices. Rubber plantation canopy heights were approximately 20 m. The
142 rubber plant rotation duration was approximately 40 yr, and the first latex tappings in this region
143 occurred when the trees were five- or six-years-old. Chemical fertilizers were applied at the initial
144 rubber plantation development stage according to local conventional farming practices. Additional
145 details regarding the rubber plantations at the experimental site can be found in the study by Sun
146 et al. (2021).

147 *2.3. Root morphological and chemical composition analysis*

148 In January 2024, three replications per depth per forest plot of soil samples with roots were
149 taken at soil depths of 0–20 and 20–40 cm, using cutting rings (200 cm³). Using the methodology
150 outlined by Chen et al. (2021), the following root features were measured: RD, root mass density
151 (RMD), RLD, and root surface area density (RSD). The cutting ring cores were placed in nylon
152 bags and taken to the laboratory, where they were submerged in water for an hour before being
153 manually washed using 0.55-mm sieves to collect the roots. The roots were scanned using an
154 Epson Perfection V800 photo scanner (© 2024 Epson America, Inc), and WinRHIZO Pro Version
155 2009c software was used to assess the RD and RL. By dividing the entire RL and root surface area
156 by the cutting-ring volume (cm³), respectively, the RLD and RSD were calculated. The roots were
157 oven-dried at 50°C, and the RMD was calculated by dividing the dry root mass by the cutting-ring

158 volume. Furthermore, using data from the WinRHIZO analyzer, the root system was classified into
159 four types based on RD: RD < 0.2 mm (very fine roots (VFRL)), RD 0.2–0.5 mm (fine roots
160 (FRL)), RD 0.5–1 mm (medium roots (MRL)), and RD > 1 mm (CRL).

161 Chemical composition (cellulose and lignin) analysis of the roots was performed on three
162 subsamples of the root classes (RD < 0.5, 0.5–1, and > 1 mm). Briefly, 1 mg of 65 °C oven-dried
163 root powder (< 0.5 mm) was mixed with 5 ml acetic acid and heated for 25 min, followed by three
164 deionized water washings and supernatant discarding. Subsequently, 10 ml of sulfuric acid (10%)
165 and 10 ml of potassium dichromic (0.1 mol L⁻¹) solutions were added, vortexed, and heated in a
166 100 °C water bath for 10 min. After cooling, 5 ml KI solution (20%) and 1 ml starch (0.5%) were
167 added, shaken for 10 min, and then titrated with 0.2 mol L⁻¹ sodium thiosulfate to determine
168 cellulose and lignin contents (Zhang et al., 2014).

169 *2.4. Soil cohesive force determination*

170 Soil samples of approximately 2000 g were collected from depths of 0–20 cm and 20–40
171 cm using a soil auger during the root collection process. The samples were carefully extracted,
172 combined, and sealed in plastic bags for transportation to the laboratory for further analysis. Soil
173 samples were air-dried and divided into two parts. One part was ground to 100 µm for SOM
174 determination using the oxidation method described by Walkley and Black (1934). The second
175 part was dry-sieved to retain aggregates < 5 mm, and visible roots were removed. These soil
176 samples were stored for subsequent analysis of the remolded soil root-free cohesion force (RFCF),
177 which was determined according to the method described by Huang et al. (2022). Briefly, four
178 subsamples ~~effor root soil composite cohesive force (RSCCF) intact root soil composite cores~~
179 were collected from each depth in three replicated plots using cutting rings (diameter = 10 cm,
180 height = 6.37 cm) simultaneously during the root collection described in Section 2.3. These intact

181 cores were used to determine soil cohesive forces. Soil cohesive force (c) was measured by
182 assessing soil shear strength (τ) and vertical load (σ) applied to the shear surface, and c was
183 calculated using the relationship between τ , σ , and c as described in Equation 1. In addition, soil
184 (< 5 mm) without visible roots was remolded into cutting rings (diameter = 10 cm, height = 6.37
185 cm) according to the soil bulk density (Table 1) at each soil depth in the rubber plots to measure
186 the soil RFCF. In total, 48 core soil samples per treatment were used for soil cohesive force
187 analysis. Both the ~~remolded root-free and root-soil composite core-RFCF and RSCCF~~ samples
188 were saturated with deionized water. After saturation, four subsamples from each depth and
189 treatment were tested using an LH-DS-4 direct shear tester (Nanjing Technology Co., Ltd.), which
190 has a shear strain accuracy of 0.01 mm and a shear stress accuracy of 0.01 N. The shear tester
191 comprised a shear box, a sensor, a vertical compression device, and a displacement measurement
192 system with specifications of 61.8 mm in diameter and a height of 20 mm. For the direct shear
193 tests, four predetermined vertical loads (25, 50, 75, and 100 kPa) were applied. The shear rate of
194 displacement was set at 0.8 ~~mm/min~~<sup>mm min⁻¹, and the soils were sheared until failure, indicated
195 by reaching the peak τ value on the computer. The relationship between the peak τ values and
196 vertical loads (σ) was established according to Mohr–Coulomb’s law, and soil cohesion (c) was
197 calculated as described in Equation 1.</sup>

$$198 \quad \tau = c + \sigma \tan\varphi \quad (1)$$

199 where τ is the soil shear strength (kPa), σ is the vertical load applied to the shear surface (kPa), c
200 is the soil cohesive force (kPa), and φ is the soil internal friction angle (°).

201 *2.5. Soil aggregate analysis*

202 Soil samples from depths of 0–20 and 20–40 cm were collected in each treatment
203 simultaneously with the root sample collection. The soil was allowed to air dry and then gently

204 ruptured along its natural cracks before it was passed through an 8 mm mesh sieve to determine
205 the soil aggregate size distribution and stability. We used a wet sieving method to separate
206 aggregates < 8 mm into four size groups: large macroaggregates (LMA) (> 2 mm);
207 macroaggregates (MA) (2–0.25 mm); microaggregates (MIA) (0.25–0.053 mm); and small
208 microaggregates (SMA) (< 0.053 mm). Briefly, three replicates of 100 g of soil were immersed in
209 deionized water for 10 min in a beaker before being transferred to a series of sieves with decreasing
210 mesh sizes (2, 0.25, and 0.053 mm) and gently shaken in water with a 4-cm vertical vibration
211 amplitude for 10 min. Subsequently, the soil that remained after each sieve was washed
212 and transferred to a beaker, and all aggregate sizes (> 2, 2–0.25, and 0.25–0.053 mm) were oven-
213 dried for 48 hours at 60 °C before being weighed. The mass of aggregates < 0.053 mm was
214 determined by subtracting the total soil mass from the total mass of other aggregate sizes (Elliott,
215 1986). Equations 2 and 3 were used to compute the mean weight diameter (MWD, mm and
216 geometric mean diameter (GMD)~~and mean weight diameter (MWD, mm)~~, respectively (Kemper
217 and Rosenau, 2018).

218
$$MWD = \sum_{i=1}^n W_i^* X_i \quad (2)$$

219 where X_i denotes the mean diameter of aggregate fraction i, and W_i denotes the mass proportion of
220 aggregate fraction i.

221
$$GMD = \exp [\sum_{i=1}^n W_i * \ln (X_i)] \quad (3)$$

222 where W_i represents the aggregate fraction mass proportion i, and X_i represents the mean diameter
223 of aggregate fraction i.

224 2.6. Statistical analysis

225 Prior to data analysis, Shapiro-Wilk ($P > 0.05$) and Levene's tests ($P > 0.05$) (Razali and
226 Wah, 2011) were used to evaluate the normality and homogeneity of variances using SPSS 25
227 (IBM Corp., Chicago, USA). ~~Origin 2021 software was used to assess each index, and Tukey's~~
228 ~~pairwise test was used to determine statistical significance at $P < 0.05, 0.01$, and 0.001 . Origin~~
229 ~~2021 software was used to evaluate each index. One-way analysis of variance (ANOVA) was~~
230 ~~conducted to determine statistical significance at $P < 0.05$, followed by Tukey's test to assess~~
231 ~~treatment significance.~~ Pearson's correlations among root characteristics, SOM, soil aggregate
232 parameters, and soil cohesive force were assessed using Origin software (OriginLab Corp.), and
233 key factors were predicted using a random forest (RF) model constructed using the R software
234 RandomForest package (v4.3.1) (Team, 2017). The partial least squares-path models (PLS-PM)
235 were performed in R software (v4.3.1) using the "plspm" package to elucidate the pathway through
236 which plant root characteristics, SOM, and soil cohesive forces influence soil aggregate stability.
237 Figures were created using Origin 2021 (OriginLab Corp.).

238 **3. Results**

239 3.1. Root distribution and chemical composition

240 Significant differences in root morphological traits were observed among rubber
241 plantations of different stand ages (Fig. 1). The RD varied notably with the age of the rubber plant
242 (Fig. 1a). The largest RD was found in 27Y_RF, followed by the MF at depths of 0–20 cm and
243 20–40 cm, respectively. Specifically, the largest RD for 27Y_RF was 0.84 mm and 0.91 mm at
244 depths of 0–20 cm and 20–40 cm, respectively. By contrast, the smallest RD, found in five-year-
245 old rubber plantations (5Y_RF), ranged from 0.42 to 0.45 mm across both depths, respectively.
246 The differences in RD among rubber plants of varying stand ages depended on soil depth, with the

247 most significant differences found at the 0–20 cm depth. Furthermore, there were notable
248 variations in RLD between rubber plantations of different stand ages, as shown in Fig. 1b..
249 27Y_RF exhibited the highest RLD, ranging from 1.83 to 2.81 $\text{cm cm}^{-3}\text{em}/\text{em}^3$, followed by MF
250 (2.01–2.06 $\text{em}/\text{em}^3\text{cm cm}^{-3}$) and 20Y_RF (1.93–2.70 $\text{em}/\text{em}^3\text{cm cm}^{-3}$) at both depths. The RLD
251 differences among rubber plants of various stand ages were influenced by soil depth, with the most
252 noticeable differences occurring at a depth of 0–20 cm. In addition, the RSD and RMD were
253 significantly different among rubber plantations of different stand ages (Fig. 1c, and d).
254 Furthermore, RD distribution, represented as a percentage of RL within each RD class, also
255 differed among rubber plantations of various stand ages (Fig. 2). In the 5Y_RF, 11Y_RF, and MF
256 plantations, VFRL (< 0.2 mm) predominated at both soil depths. Conversely, in the 20Y_RF and
257 27Y_RF plantations, the roots were uniformly distributed across the soil depths, with a relatively
258 high percentage of MRL (0.5–1 mm).

259 The root chemical composition varied among rubber plantations of different stand ages and
260 RD classes (Fig. 3). The cellulose contents in stand-age rubber plants were significantly different
261 (Fig. 3a). The 20Y_RF roots had higher cellulose content than those of the 27Y_RF, followed by
262 the 11Y_RF. Similarly, cellulose content varied across the RD classes, with the 5Y_RF having
263 lower cellulose levels than other stand-age rubber plants for FRL (< 0.5 mm). Moreover, there
264 were significant differences in lignin content among the stand-age rubber plants and between the
265 RD classes (Fig. 3b). For example, the lignin contents in the 20Y_RF were less than that in the
266 5Y_RF for RL < 0.5 mm. Cellulose and lignin contents are indicators of root contribution to SOM.
267 Thus, the lower lignin and higher cellulose content in the 20Y_RF resulted in the highest SOM
268 content ranging from 21.16 to 23.37 g/kg, followed by that in the 11Y_RF ranging from 20.56 to
269 22.68 $\text{g/kg}\text{g kg}^{-1}$, and the 27Y_RF ranging from 21.04 to 21.78 g/kg within soil depth (Fig. 3c).

270 3.2. *Soil cohesive force under different stand-age rubber plantations*

271 There was a significant difference in the RFCF among rubber plantations of different stand
272 ages (Fig. 4a). The CK (without plants) RFCF was 17.92 and 20.25 kPa at depths of 0–20 and 20–
273 40 cm, respectively, and the RFCF matric significantly increased with the introduction of rubber
274 plantations of different stand ages. For example, at 0–10 cm soil depth, compared to the CK, the
275 ability of rubber plants to improve the soil cohesive force followed the order MF > 27Y_RF >
276 20Y_RF > 11Y_RF > 5Y_RF. For the 20Y_RF, the increases in RFCFs relative to the CK were
277 169.73 and 156 % at 0–20 and 20–40 cm, respectively. Generally, older rubber plants (> 11-years-
278 old) yielded a greater RFCF than younger rubber plants.

279 The root–soil composite cohesive force exhibited different patterns among rubber
280 plantations of different stand ages compared to that of the RFCF (Fig. 4b). The root–soil composite
281 cohesive force showed significant differences among rubber plantations of different stand ages and
282 with that in the CK at 0–20 cm depths, whereas the root–soil composite force was significantly
283 greater with plants than with that in the CK at 20–40 cm depth. However, there were no significant
284 differences in the root–soil composite cohesive forces among the different plantations within the
285 20–40 cm soil depth. This is likely because rubber plants of different stand ages (20Y_RF, 27Y_RF,
286 and MF) had greater root–soil interactions, likely due to thicker RD, higher RLD, higher
287 percentage of MRL, and higher SOM at a depth of 0–20 cm. Overall, both cohesive forces were
288 significantly correlated with RLD, VFRL, FRL, and SOM (Fig. 6). These results indicate that
289 rubber plantations of different stand ages have a greater ability to improve soil cohesive forces.

290 3.3. *Soil aggregate properties under different stand-age rubber plantations*

291 Soil aggregate properties exhibited different patterns among the various rubber plant
292 treatments (Fig. 5). Soil aggregates sizes were predominantly 2–0.25 mm, followed by > 2 mm,

293 and 0.25–0.053 mm, and aggregate sizes > 0.053 mm were less dominant in all rubber plantations
294 of different stand ages compared to that in the CK at the respective soil depths (Fig. 5a–f). In the
295 CK, the 2–0.025 mm aggregates accounted for 23.76% at a depth of 0–20 cm and 26.84% at 20–
296 40 cm. Compared to the CK, rubber plantations of different stand ages showed a significant
297 increase in 2–0.25 mm aggregates at both soil depths. However, the proportion of aggregates > 2
298 mm, significantly increased in rubber plantations of different stand ages compared to that in the
299 CK at respective soil depths, in the order 20Y_RF $>$ 11Y_RF $>$ 27Y_RF $>$ MF $>$ 5Y_RF.
300 Simultaneously, the proportion of aggregates < 0.053 mm was significantly reduced in rubber
301 plantations of different stand ages compared with the CK. The increase in macroaggregates (> 2
302 mm) and decrease in microaggregates (< 0.053 mm) following rubber plantation treatments of
303 varying stand ages led to improvements in aggregate stability (measured by MWD and GMD) in
304 the following order: 20Y_RF $>$ 27Y_RF $>$ 11Y_RF $>$ MF $>$ 5Y_RF $>$ CK.

305 *3.4 Relationship among root traits, SOM, cohesive force, and soil aggregate stability*

306 The Pearson correlation analysis revealed a strong positive correlation between soil RFCF
307 and MWD as well as GMD, with correlation coefficients of 0.81 and 0.91 (0–20 cm) and 0.81 and
308 0.89 (20–40 cm). In contrast, soil RFCF showed a significant negative correlation with small
309 microaggregates (< 0.053 mm), with correlation values of -0.74 and -0.79 at both depths (Fig. 6).
310 A similar pattern was observed for the root–soil composite cohesive force. In general, a stronger
311 cohesive force was associated with higher RLD, greater proportions of FRL and MRL, and higher
312 SOM, especially in older rubber plants, which contributed to their ability to maintain greater
313 aggregate stability.

314 The Random Forest (RF) model highlighted the significance of various soil factors in
315 predicting soil aggregate stability (MWD and GMD) across both soil depths (Fig. 7), with LMA

316 (>2 mm) and MA (2–0.25 mm) emerging as the most influential contributors to stability, followed
317 by SOM and FRL (FRL_0.2–0.5 mm). Root properties and soil cohesive forces also play
318 substantial roles, particularly at deeper soil depths (20–40 cm), where cohesive forces become
319 more prominent. ~~Root traits are essential for enhancing soil aggregate stability, and their impact~~
320 ~~varies with depth, underscoring the complex interactions between roots and soil structure in~~
321 ~~ecosystem functions.~~ Furthermore, the PLS-PM clarified both the direct and indirect effects of root
322 properties, SOM, and cohesive forces on soil aggregate stability (Fig. 8). Among the factors
323 measured in the surface soil (0–20 cm), RLD (path coefficient 0.64, $P < 0.05$) directly influenced
324 SOM (path coefficient 0.45, $P < 0.05$) and the MWD. In addition, RLD had a strong direct effect
325 on SOM (path coefficient 0.70, $P < 0.05$). Furthermore, RLD directly altered RFCF (path
326 coefficient 0.30, $P < 0.05$), which further affected the MWD. In contrast, RLD directly influenced
327 the ~~root soil composite cohesive force (RSCCF)~~, however, the RSCCF did not directly influence
328 the MWD. A similar trend was observed in the deep soil (20–40 cm).

329 **4. Discussion**

330 *4.1. Stand-age rubber plant root influence on soil cohesive forces*

331 Rubber plantations of different stand ages exhibited different root morphological traits.
332 Our results demonstrated that the plant roots of rubber plantations aged < 11-years-old were
333 influenced by soil properties at 0–20 and 20–40 cm depths, as indicated by a sharp decline in RD
334 and RLD (Fig. 1), and restricted root growth due to an increase in soil bulk density and a decrease
335 in macropores. Similarly, Sun et al. (2021) observed that at the same research site, older rubber
336 plants (13-years-old) exhibited a preference for growing in macropores compared to younger
337 plants (four-years-old), which was attributed to their superior root properties and lower soil bulk
338 density. In contrast, the 27Y_RF and MF were minimally influenced by soil properties due to the

339 high percentage of FRL and MRL, which likely enlarged medium soil pores and facilitated
340 penetration through capillary soil pores ($< 30 \mu\text{m}$) (Ali et al., 2022; Chen et al., 2021; He et al.,
341 2022). Older rubber plants possess a higher proportion of FRL and MRL and produce a greater
342 amount of root exudates, which likely function as lubricants to facilitate root growth in compacted
343 soils with a higher bulk density (Chen et al., 2017; Sun et al., 2023). In our study, older rubber
344 plants demonstrated a higher root penetration ability than younger plants, which likely modified
345 the soil cohesive forces.

346 Our results indicate that rubber plant roots of different stand ages were more effective in
347 enhancing soil cohesive forces in tropical regions than in the CK (no rubber plants) (Fig. 4). Many
348 studies have highlighted that plant roots enhance soil detachment resistance during rainfall events,
349 primarily by increasing soil cohesive forces (Huang et al., 2022; Shen et al., 2021). Our findings
350 further confirm that rubber plantations of different stand ages generate varying soil cohesive forces,
351 which are influenced by their root properties and contributions to SOM. The differences in the
352 enhancement of root–soil composite cohesive forces among rubber plantations of varying stand
353 ages were attributed to their distinct root properties. Younger rubber plants ($< 20\text{Y_RF}$) were more
354 effective at increasing soil cohesion in the topsoil (0–20 cm), whereas older plants improved soil
355 cohesion in both the topsoil and deeper layers compared to that in the CK (Fig. 4) because of their
356 higher root tensile strength, soil shear strength, and greater RD and RLD. However, the RD and
357 RLD of younger plants were significantly reduced in the subsoil, thereby diminishing their impact
358 on soil cohesion. In contrast, older rubber plants enhance soil cohesive forces because of their
359 extensive root contact area with the soil and the high density of their crisscrossing FRL and MRL
360 networks, which effectively bind and wrap soil particles (Huang et al., 2022; Vannoppen et al.,

361 2015–; 2017). In the current study, RLD and a substantial proportion of FRL and MRL in older
362 rubber plants enhanced root–soil contact and strengthened the soil at both depths (Figs. 1, and 2).

363 The impact of roots on the cohesive force of root-free soils can be attributed to their indirect
364 contribution to ~~soil organic matter~~ (SOM). Soils from older rubber plantations, which exhibited
365 higher SOM content (Fig. 3c), enhanced clay particle cohesion by reducing the surface tension of
366 water within the clay–organic matter matrix (Wuddivira et al., 2009). RD and chemical
367 composition (cellulose) altered carbon sequestration in various soil pools, enhancing carbon
368 accumulation in the coarse silt fraction (20–50 μm), while decreasing carbon accumulation in
369 particulate organic matter (Liao et al., 2023; Zhang et al., 2014). Similarly, roots with higher
370 cellulose-to-lignin ratios improve substrate availability for polymer-hydrolyzing enzymes, thereby
371 speeding up the degradation of plant organic ~~materials matter~~—(Barto et al., 2010; Halder et al.,
372 2021; Zhang et al., 2014). In addition, root exudates facilitate root penetration into compacted soil
373 layers and increase the distribution frequency of SOM in deeper soil horizons (Oleghe et al., 2017).
374 In general, older rubber plants exhibited a greater RLD, higher percentage of FRL and MRL, and
375 increased SOM than younger rubber plants, which led to a higher RFCF.

376 *4.2. Aggregate stability responses to soil cohesive forces under different stand-age rubber*
377 *plantations*

378 Our study provides comprehensive insights into soil aggregate stability across rubber
379 plantations at different stages of stand maturity. Soil cohesive forces driven by plant root traits are
380 key factors in enhancing soil aggregate stability. The soil cohesive force increased aggregate
381 stability (MWD and GMD) at the same soil depth (Fig. 5). The root morphology traits like fine
382 FRL, CRL, RD, RLD, influence the soil cohesive force and binding of soil particles and then
383 indirectly increase aggregate stability (MWD and GMD). The results also indicated that cohesive
384 forces not only governed macroaggregate stability but also played a role in microaggregate

385 formation. Macroaggregates are primarily stabilized by cohesive forces derived from organic
386 matter, root exudates, and fungal hyphae. In our study, the significant increase in RFCF with the
387 introduction of rubber plantations (Fig. 4a) indicates that cohesive forces are enhanced by root
388 activity and organic matter inputs. Similarly, microaggregates are formed through the binding of
389 primary particles (clay, silt, and fine organic matter) by cohesive forces. In our study, the increased
390 RFCF in older plantations (Fig. 4a) suggests that cohesive forces are strong enough to facilitate
391 the formation of microaggregates, particularly in the topsoil (0–20 cm depth). The MWD increased
392 across rubber plantations of different stand ages because of the significant enhancement in soil
393 cohesive forces. Rubber plants older than 11 years exhibited the highest aggregate stability at the
394 same soil depth, which was consistent with the trend observed in their RFCF (Fig. 4). High soil
395 cohesion has also been documented to limit soil dispersion rates and mitigate gully erosion
396 (Wuddivira et al., 2013). Although the soil RFCCF was highest in older rubber plantations, the
397 highest SOM content likely played a positive role in stabilizing soil particles (Kamau et al., 2020).
398 SOM influences soil particles in several ways, primarily by enhancing soil aggregation and
399 improving soil structure. SOM contributes to the formation of aggregates by acting as a binding
400 agent between soil particles, especially through its interaction with clay minerals and other soil
401 constituents. The organic compounds in SOM help form cohesive forces that promote the
402 flocculation of fine soil particles, creating larger, more stable aggregates. SOM had a positive
403 effect on soil particles as its dispersive properties became evident only once the soil aggregates
404 were broken down. High SOM content also weakens the electrostatic repulsive forces by
405 influencing the overlap of oppositely charged electric double layers (Ali et al., 2023; Yu et al.,
406 2020). In addition, the higher MWD observed in rubber plantations older than 11 years, compared
407 to those in the 5Y_RF and CK, indicated that the MWD of older rubber plants was not adversely

408 affected by the excessive release of SOC from the mechanical breakdown of macroaggregates.
409 During this breakdown process, the enhanced root biomass and higher SOM content in older
410 rubber plantations help stabilize soil aggregates and mitigate the adverse effects of SOC loss.
411 Additionally, ~~the~~ higher RLD and root-derived SOM in older plantations promote microaggregate
412 formation, further supporting aggregate stability and contributing to the observed increase in
413 MWD, despite the release of some SOC from macroaggregate breakdown.

414 These findings highlight the importance of understanding the specific mechanisms by
415 which soil cohesive forces contribute to aggregate stability. In this study, the soil aggregate portion
416 (< 0.25 mm) was comparatively higher in the rubber plantations than in the control in this study.
417 Rubber plant roots and SOM positively enhanced cohesion between soil particles (Fig. 5a–f). The
418 soil cohesive force regulates soil aggregate stability using the following approaches. ~~First~~, smaller
419 aggregates, due to their higher surface area to volume ratio with water, can create surface tension
420 between particles, indirectly creating a cohesive force, helping to hold them together (Wang et al.,
421 2023). Second, soil particles, particularly clay and organic matter, often carry electrical charges
422 that can lead to electrostatic attraction, further stabilizing the soil particles (Kaiser and Asefaw
423 ~~Berhe~~, 2014; Wuddivira et al., 2009). ~~Similarly~~, SOM has a positive effect on clays because the
424 dispersive effect of SOM is not expressed until the aggregates are broken (Melo et al., 2021). High
425 SOM also weakens the electrostatic repulsive force in ultisols through its additional impact on the
426 overlap of oppositely charged electric double layers (Ali et al., 2023; He et al., 2021; Yu et al.,
427 2020). Third, the water in the small pores between the soil particles creates a capillary force that
428 contributes to the soil cohesive force, which agglomerates the small particles (Deviren Saygin et
429 al., 2021). In general, stand-age rubber plantations positively improved soil aggregate stability
430 compared to the control through soil cohesion. In young rubber plantations, legumes such as kudzu

431 should be planted. Furthermore, the development of a forest rubber understory economy can
432 significantly enhance soil health by increasing biodiversity, with diverse plant roots improving soil
433 structure, promoting microbial activity, preventing erosion, and contributing to organic matter
434 through leaf litter and root biomass, thereby improving soil fertility. Future research should focus
435 on evaluating the mechanisms by which various understory plants in rubber plantations reduce soil
436 erosion.

437 **5. Conclusion**

438 In this study, we investigated how root morphological traits, root-derived SOM, and the
439 chemical composition of rubber plants at different stand ages influence soil aggregate stability
440 through soil cohesive forces. Our findings indicate that natural rubber plantations of different stand
441 ages exhibit distinct root distribution patterns, with older rubber plantations, particularly 27-year-
442 old rubber forests, and MF demonstrating a more developed root system characterized by greater
443 RLD and higher proportions of FRL and MRL diameter classes compared to younger plantations.
444 The higher percentages of FRL and MRL in older rubber plants (> 11 years old), along with their
445 high SOM content, contributed to a stronger soil cohesive force than that observed in younger
446 rubber plants and the control plots. The higher SOM content in older rubber plants was driven by
447 the higher cellulose content and lower lignin percentages in their FRL and MRL. Consequently,
448 rubber plants older than 11 years increased the soil cohesive force (with and without roots)
449 compared to younger rubber plants and the control, thereby enhancing aggregate stability and
450 reducing soil particle dispersion. ~~These findings have valuable practical implications for~~
451 ~~developing management strategies to restore soil quality in degraded tropical regions of Hainan~~
452 ~~Island. They highlight the importance of selecting rubber plants with ideal root traits to improve~~
453 ~~aggregate stability through soil cohesive forces, ensuring long-term agricultural productivity and~~

454 preserving environmental quality. These findings offer practical implications for managing rubber
455 plantations across different stand ages to restore soil quality in degraded tropical regions of Hainan
456 Island. For instance, younger stands may benefit from targeted organic amendments or
457 intercropping to accelerate SOM accumulation, while older stands might require interventions to
458 mitigate aggregate breakdown through root properties. The study underscores the role of root
459 systems in soil stability, suggesting that management practices promoting robust root development
460 regardless of variety could enhance aggregate cohesion and long-term productivity.

461 **Credit authorship contribution statement**

462 **WA:** Writing - original draft, visualization, Investigation, Data curation, formal analysis. **AM**
463 Investigation, Data curation. **TL:** visualization, formal analysis, **NK:** Writing – review & editing.
464 **AS:** Writing – review & editing. **KS:** Investigation, formal analysis. **QY:** Investigation, Funding
465 acquisition, review & editing. **HY:** Writing – review & editing, **WL:** Investigation, Data curation.
466 **WL:** Validation, Supervision, Resources, Conceptualization, Funding acquisition.

467 **Declaration of Competing Interest**

468 The authors declare that they have no known competing financial interests or personal
469 relationships that could have appeared to influence the work reported in this paper.

470 **Data availability**

471 Data will be made available on request.

472 **Acknowledgment**

473 This work was financially supported by the , National Key Research and Development Program
474 of China (2021YFD2200403-04), Hainan Province Postdoctoral Research Project
475 (RZ2500001086) and the National Natural Science Foundation of China (No. 42367034 and
476 32160291).

477 **References**

478 Ali, W., Yang, M., Long, Q., Hussain, S., Chen, J., Clay, D., and He, Y.: Different fall/winter
479 cover crop root patterns induce contrasting red soil (Ultisols) mechanical resistance through
480 aggregate properties, *Plant and Soil*, 477, 461–474, <https://doi.org/10.1007/s11104-022-05430-4>,
481 2022.

482 Ali, W., Hussain, S., Chen, J., Hu, F., Liu, J., He, Y., and Yang, M.: Cover crop root-derived
483 organic carbon influences aggregate stability through soil internal forces in a clayey red soil,
484 *Geoderma*, 429, 116271, <https://doi.org/10.1016/j.geoderma.2022.116271>, 2023.

485 Barto, E. K., Alt, F., Oelmann, Y., Wilcke, W., and Rillig, M. C.: Contributions of biotic and
486 abiotic factors to soil aggregation across a land use gradient, *Soil Biology and Biochemistry*, 42,
487 2316–2324, <https://doi.org/10.1016/j.soilbio.2010.09.008>, 2010.

488 Chen, C., Liu, W., Jiang, X., and Wu, J.: Effects of rubber-based agroforestry systems on soil
489 aggregation and associated soil organic carbon: Implications for land use, *Geoderma*, 299, 13–24,
490 <https://doi.org/10.1016/j.geoderma.2017.03.021>, 2017.

491 Chen, J., Wu, Z., Zhao, T., Yang, H., Long, Q., and He, Y.: Rotation crop root performance and
492 its effect on soil hydraulic properties in a clayey Utisol, *Soil and Tillage Research*, 213, 105136,
493 <https://doi.org/10.1016/j.still.2021.105136>, 2021.

494 Deviren Saygin, S., Arı, F., Temiz, Ç., Arslan, Ş., Ünal, M. A., and Erpul, G.: Analysis of soil
495 cohesion by fluidized bed methodology using integrable differential pressure sensors for a wide
496 range of soil textures, *Computers and Electronics in Agriculture*, 191,
497 <https://doi.org/10.1016/j.compag.2021.106525>, 2021.

498 Elliott, E. T.: Aggregate Structure and Carbon, Nitrogen, and Phosphorus in Native and Cultivated
499 Soils, *Soil Science Society of America Journal*, 50, 627–633,

500 https://doi.org/10.2136/sssaj1986.0361599500500030017x, 1986.

501 Forster, M., Ugarte, C., Lamandé, M., and Faucon, M.-P.: Root traits of crop species contributing

502 to soil shear strength, *Geoderma*, 409, 115642, https://doi.org/10.1016/j.geoderma.2021.115642,

503 2022.

504 Halder, M., Liu, S., Zhang, Z. B., Guo, Z. C., and Peng, X. H.: Effects of residue stoichiometric,

505 biochemical and C functional features on soil aggregation during decomposition of eleven organic

506 residues, *CATENA*, 202, 105288, https://doi.org/10.1016/j.catena.2021.105288, 2021.

507 He, Y., Yang, M., Huang, R., Wang, Y., and Ali, W.: Soil organic matter and clay zeta potential

508 influence aggregation of a clayey red soil (Ultisol) under long-term fertilization, *Scientific Reports*,

509 11, 20498, https://doi.org/10.1038/s41598-021-99769-w, 2021.

510 He, Y., Wu, Z., Zhao, T., Yang, H., Ali, W., and Chen, J.: Different plant species exhibit

511 contrasting root traits and penetration to variation in soil bulk density of clayey red soil, *Agronomy*

512 *Journal*, 114, 867–877, https://doi.org/10.1002/agj2.20972, 2022.

513 Hok, L., de Moraes Sá, J. C., Boulakia, S., Reyes, M., de Oliveira Ferreira, A., Elie Tivet, F., Saab,

514 S., Auccaise, R., Massao Inagaki, T., Schimiguel, R., Aparecida Ferreira, L., Briedis, C., Santos

515 Canalli, L. B., Kong, R., and Leng, V.: Dynamics of soil aggregate-associated organic carbon

516 based on diversity and high biomass-C input under conservation agriculture in a savanna

517 ecosystem in Cambodia, *CATENA*, 198, 105065, https://doi.org/10.1016/j.catena.2020.105065,

518 2021.

519 Huang, M., Sun, S., Feng, K., Lin, M., Shuai, F., Zhang, Y., Lin, J., Ge, H., Jiang, F., and Huang,

520 Y.: Effects of *Neyraudia reynaudiana* roots on the soil shear strength of collapsing wall in

521 Benggang, southeast China, *Catena*, 210, 105883, https://doi.org/10.1016/j.catena.2021.105883,

522 2022

523 Kaiser, M. and Asefaw Berhe, A.: How does sonication affect the mineral and organic constituents
524 of soil aggregates? - A review, *Journal of Plant Nutrition and Soil Science*, 177, 479–495,
525 <https://doi.org/10.1002/jpln.201300339>, 2014.

526 Kamau, S., Barrios, E., Karanja, N. K., Ayuke, F. O., and Lehmann, J.: Dominant tree species and
527 earthworms affect soil aggregation and carbon content along a soil degradation gradient in an
528 agricultural landscape, *Geoderma*, 359, 113983, <https://doi.org/10.1016/j.geoderma.2019.113983>,
529 2020.

530 Kemper, W. D. and Rosenau, R. C.: Aggregate Stability and Size Distribution, in: *Agronomy*
531 Monograph, vol. 9, 425–442, <https://doi.org/10.2136/sssabookser5.1.2ed.c17>, 2018.

532 Kumar, A., Dorodnikov, M., Splettstößer, T., Kuzyakov, Y., and Pausch, J.: Effects of maize roots
533 on aggregate stability and enzyme activities in soil, *Geoderma*, 306, 50–57,
534 <https://doi.org/10.1016/j.geoderma.2017.07.007>, 2017.

535 Kurmi, B., Nath, A. J., Lal, R., and Das, A. K.: Water stable aggregates and the associated active
536 and recalcitrant carbon in soil under rubber plantation, *Science of the Total Environment*, 703,
537 135498, <https://doi.org/10.1016/j.scitotenv.2019.135498>, 2020.

538 Li, T., Hong, X., Liu, S., Wu, X., Fu, S., Liang, Y., Li, J., Li, R., Zhang, C., Song, X., Zhao, H.,
539 Wang, D., Zhao, F., Ruan, Y., and Ju, X.: Cropland degradation and nutrient overload on Hainan
540 Island: A review and synthesis, *Environmental Pollution*, 313, 120100,
541 <https://doi.org/10.1016/j.envpol.2022.120100>, 2022.

542 Liao, J., Yang, X., Dou, Y., Wang, B., Xue, Z., Sun, H., Yang, Y., and An, S.: Divergent
543 contribution of particulate and mineral-associated organic matter to soil carbon in grassland,
544 *Journal of Environmental Management*, 344, 118536,
545 <https://doi.org/https://doi.org/10.1016/j.jenvman.2023.118536>, 2023.

546 Melo, T. R. de, Figueiredo, A., and Filho, J. T.: Clay behavior following macroaggregate
547 breakdown in Ferralsols, Soil and Tillage Research, 207, 104862,
548 <https://doi.org/10.1016/j.still.2020.104862>, 2021.

549 Nornadiah Mohd Razali Yap Bee Wah: Power comparisons of Shapiro-Wilk, Kolmogorov-
550 Smirnov, Lilliefors and Anderson-Darling tests, Journal of Statistical Modeling and Analytics, 21–
551 33, 2011.

552 Oleghe, E., Naveed, M., Baggs, E. M., and Hallett, P. D.: Plant exudates improve the mechanical
553 conditions for root penetration through compacted soils, Plant and Soil, 421, 19–30,
554 <https://doi.org/10.1007/s11104-017-3424-5>, 2017.

555 Perović, V., Kadović, R., Đurđević, V., Pavlović, D., Pavlović, M., Čakmak, D., Mitrović, M., and
556 Pavlović, P.: Major drivers of land degradation risk in Western Serbia: Current trends and future
557 scenarios, Ecological Indicators, 123, 107377, <https://doi.org/10.1016/j.ecolind.2021.107377>,
558 2021.

559 Poirier, V., Roumet, C., Angers, D. A., and Munson, A. D.: Species and root traits impact
560 macroaggregation in the rhizospheric soil of a Mediterranean common garden experiment, Plant
561 and Soil, 424, 289–302, <https://doi.org/10.1007/s11104-017-3407-6>, 2018a.

562 Poirier, V., Roumet, C., and Munson, A. D.: The root of the matter: Linking root traits and soil
563 organic matter stabilization processes, Soil Biology and Biochemistry, 120, 246–259,
564 <https://doi.org/10.1016/j.soilbio.2018.02.016>, 2018b.

565 Prăvălie, R., Nita, I.-A., Patriche, C., Niculiță, M., Birsan, M.-V., Roșca, B., and Bandoc, G.:
566 Global changes in soil organic carbon and implications for land degradation neutrality and climate
567 stability, Environmental Research, 201, 111580, <https://doi.org/10.1016/j.envres.2021.111580>,
568 2021.

569 Rabot, E., Wiesmeier, M., Schlüter, S., and Vogel, H.-J.: Soil structure as an indicator of soil
570 functions: A review, *Geoderma*, 314, 122–137, <https://doi.org/10.1016/j.geoderma.2017.11.009>,
571 2018.

572 Rossi, L. M. W., Mao, Z., Merino-Martín, L., Roumet, C., Fort, F., Taugourdeau, O., Boukcim,
573 H., Fourtier, S., Del Rey-Granado, M., Chevallier, T., Cardinael, R., Fromin, N., and Stokes, A.:
574 Pathways to persistence: plant root traits alter carbon accumulation in different soil carbon pools,
575 *Plant and Soil*, 452, 457–478, <https://doi.org/10.1007/s11104-020-04469-5>, 2020.

576 Schad, P.: World Reference Base for Soil Resources—Its fourth edition and its history, *Journal of
577 Plant Nutrition and Soil Science*, 186, 151–163, <https://doi.org/10.1002/jpln.202200417>, 2023.

578 Shao, W., Zhang, Z., Guan, Q., Yan, Y., and Zhang, J.: Comprehensive assessment of land
579 degradation in the arid and semiarid area based on the optimal land degradation index model,
580 *CATENA*, 234, 107563, <https://doi.org/10.1016/j.catena.2023.107563>, 2024.

581 Shen, N., Wang, Z., Guo, Q., Zhang, Q., Wu, B., Liu, J., Ma, C., Delang, C. O., and Zhang, F.:
582 Soil detachment capacity by rill flow for five typical loess soils on the Loess Plateau of China,
583 *Soil and Tillage Research*, 213, 105159, <https://doi.org/10.1016/j.still.2021.105159>, 2021.

584 Smith, D. J., Wynn-Thompson, T. M., Williams, M. A., and Seiler, J. R.: Do roots bind soil?
585 Comparing the physical and biological role of plant roots in fluvial streambank erosion: A mini-
586 JET study, *Geomorphology*, 375, 107523, <https://doi.org/10.1016/j.geomorph.2020.107523>, 2021.

587 Sun, R., Wu, Z., Lan, G., Yang, C., and Fraedrich, K.: Effects of rubber plantations on soil
588 physicochemical properties on Hainan Island, China, *Journal of Environmental Quality*, 50, 1351–
589 1363, <https://doi.org/10.1002/jeq2.20282>, 2021.

590 Sun, R., Lan, G., Yang, C., Wu, Z., Chen, B., and Fraedrich, K.: Soil quality variation and its
591 driving factors within tropical forests on Hainan Island, China, *Land Degradation and*

592 Development, 34, 3418–3432, <https://doi.org/10.1002/ldr.4693>, 2023.

593 Team, R. C.: a Language and Environment for Statistical Computing, 2017.

594 Thomas, A., Bentley, L., Feeney, C., Loftis, S., Robb, C., Rowe, E. C., Thomson, A., Warren-

595 Thomas, E., and Emmett, B.: Land degradation neutrality: Testing the indicator in a temperate

596 agricultural landscape, Journal of Environmental Management, 346, 118884,

597 <https://doi.org/10.1016/j.jenvman.2023.118884>, 2023.

598 Vannoppen, W., Vanmaercke, M., De Baets, S., and Poesen, J.: A review of the mechanical effects

599 of plant roots on concentrated flow erosion rates, Earth-Science Reviews, 150, 666–678,

600 <https://doi.org/10.1016/j.earscirev.2015.08.011>, 2015.

601 Vannoppen, W., De Baets, S., Keeble, J., Dong, Y., and Poesen, J.: How do root and soil

602 characteristics affect the erosion-reducing potential of plant species?, Ecological Engineering, 109,

603 186–195, <https://doi.org/10.1016/j.ecoleng.2017.08.001>, 2017.

604 Walkley, A. and Black, I. A.: An examination of the degtjareff method for determining soil organic

605 matter, and a proposed modification of the chromic acid titration method, Soil Science, 37, 29–38,

606 <https://doi.org/10.1097/00010694-193401000-00003>, 1934.

607 Wang, B., Zhang, G.-H., Yang, Y.-F., Li, P.-P., and Liu, J.-X.: Response of soil detachment

608 capacity to plant root and soil properties in typical grasslands on the Loess Plateau, Agriculture,

609 Ecosystems & Environment, 266, 68–75, <https://doi.org/10.1016/j.agee.2018.07.016>, 2018a.

610 Wang, B., Zhang, G.-H., Yang, Y.-F., Li, P.-P., and Liu, J.-X.: The effects of varied soil properties

611 induced by natural grassland succession on the process of soil detachment, CATENA, 166, 192–

612 199, <https://doi.org/10.1016/j.catena.2018.04.007>, 2018b.

613 Wang, G., Huang, Y., Li, R., Chang, J., and Fu, J.: Influence of Vetiver Root System on

614 Mechanical Performance of Expansive Soil: Experimental Studies, Advances in Civil Engineering,

615 2020, 1–11, <https://doi.org/10.1155/2020/2027172>, 2020a.

616 Wang, G. Y., Huang, Y. G., Li, R. F., Chang, J. M., and Fu, J. L.: Influence of vetiver root on
617 strength of expansive soil-experimental study, PLoS ONE, 15, 1–20,
618 <https://doi.org/10.1371/journal.pone.0244818>, 2020b.

619 Wang, J., Wei, H., Huang, J., He, T., and Deng, Y.: Soil aggregate stability and its response to
620 overland runoff–sediment transport in karst peak–cluster depressions, Journal of Hydrology, 620,
621 129437, <https://doi.org/10.1016/j.jhydrol.2023.129437>, 2023.

622 Wuddivira, M. N., Stone, R. J., and Ekwue, E. I.: Clay, Organic Matter, and Wetting Effects on
623 Splash Detachment and Aggregate Breakdown under Intense Rainfall, Soil Science Society of
624 America Journal, 73, 226–232, <https://doi.org/10.2136/sssaj2008.0053>, 2009.

625 Wuddivira, M. N., Stone, R. J., and Ekwue, E. I.: Influence of cohesive and disruptive forces on
626 strength and erodibility of tropical soils, Soil and Tillage Research, 133, 40–48,
627 <https://doi.org/10.1016/j.still.2013.05.012>, 2013.

628 Xu, W., Liu, W., Tang, S., Yang, Q., Meng, L., Wu, Y., Wang, J., Wu, L., Wu, M., Xue, X., Wang,
629 W., and Luo, W.: Long-term partial substitution of chemical nitrogen fertilizer with organic
630 fertilizers increased SOC stability by mediating soil C mineralization and enzyme activities in a
631 rubber plantation of Hainan Island, China, Applied Soil Ecology, 182, 104691,
632 <https://doi.org/10.1016/j.apsoil.2022.104691>, 2023.

633 Yang, Q., Li, J., Xu, W., Wang, J., Jiang, Y., Ali, W., and Liu, W.: Substitution of Inorganic
634 Fertilizer with Organic Fertilizer Influences Soil Carbon and Nitrogen Content and Enzyme
635 Activity under Rubber Plantation, Forests, 15, 756, <https://doi.org/10.3390/f15050756>, 2024.

636 Yu, Z., Zheng, Y., Zhang, J., Zhang, C., Ma, D., Chen, L., and Cai, T.: Importance of soil
637 interparticle forces and organic matter for aggregate stability in a temperate soil and a subtropical

638 soil, *Geoderma*, 362, 114088, <https://doi.org/10.1016/j.geoderma.2019.114088>, 2020.

639 Yudina, A. and Kuzyakov, Y.: Dual nature of soil structure: The unity of aggregates and pores,

640 *Geoderma*, 434, 116478, <https://doi.org/10.1016/j.geoderma.2023.116478>, 2023.

641 Zhang, C.-B., Chen, L.-H., and Jiang, J.: Why fine tree roots are stronger than thicker roots: The

642 role of cellulose and lignin in relation to slope stability, *Geomorphology*, 206, 196–202,

643 <https://doi.org/10.1016/j.geomorph.2013.09.024>, 2014.

644 Zhu, X., Liu, W., Yuan, X., Chen, C., Zhu, K., Zhang, W., and Yang, B.: Aggregate stability and

645 size distribution regulate rainsplash erosion: Evidence from a humid tropical soil under different

646 land-use regimes, *Geoderma*, 420, 115880, <https://doi.org/10.1016/j.geoderma.2022.115880>,

647 2022.

648 Zou, X., Zhu, X., Zhu, P., Singh, A. K., Zakari, S., Yang, B., Chen, C., and Liu, W.: Soil quality

649 assessment of different *Hevea brasiliensis* plantations in tropical China, *Journal of Environmental*

650 *Management*, 285, 112147, <https://doi.org/10.1016/j.jenvman.2021.112147>, 2021.

651

652

653

654

655

656

657

658

659

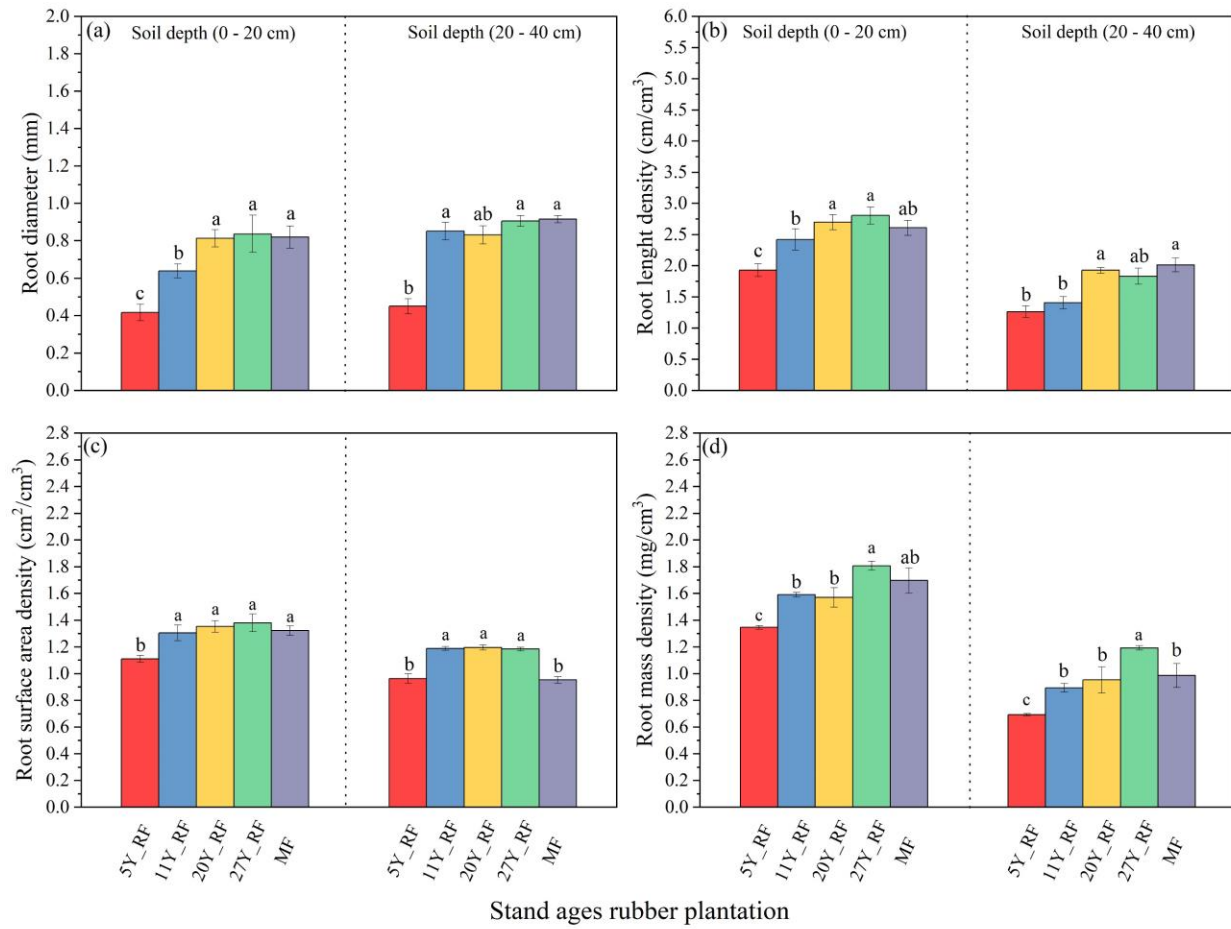
660

661 **Table captions**662 **Table. 1.** Basic physical and chemical characteristics of the experimental site.

Treatments	Soil depth (cm)	pH	BD (g/cm ³)	TOP (%)	SMC (%)	SOM (g/kg)	AN (mg/kg)	AP (mg/kg)	AK (mg/kg)
CK	0 - 20	4.17	1.52	26.37	17.46	12.34	11.92	1.69	24.42
	20 - 40	4.21	1.56	23.26	15.25	11.36	11.45	1.56	18.15
5Y_RF	0 - 20	4.37	1.39	28.39	19.25	20.98	11.63	2.79	34.62
	20 - 40	4.13	1.52	23.01	17.63	16.30	10.67	1.73	17.97
11Y_RF	0 - 20	3.89	1.43	24.81	21.67	22.68	11.84	2.31	25.23
	20 - 40	4.02	1.51	23.1	20.77	20.56	10.42	1.7	16.44
20Y_RF	0 - 20	4.08	1.36	24.98	21.41	23.37	10.67	2.33	29.02
	20 - 40	4.22	1.43	20.31	20.2	21.16	10.39	1.99	23.12
27Y_RF	0 - 20	4.08	1.32	25.05	23.68	21.78	11.77	2.39	25.83
	20 - 40	4.26	1.41	25.24	19.9	21.04	10.17	1.84	18.92
MF	0 - 20	4.42	1.31	29.52	22.76	21.20	13.47	1.81	36.15
	20 - 40	4.35	1.39	26.58	20.11	20.29	12.84	1.33	19.94

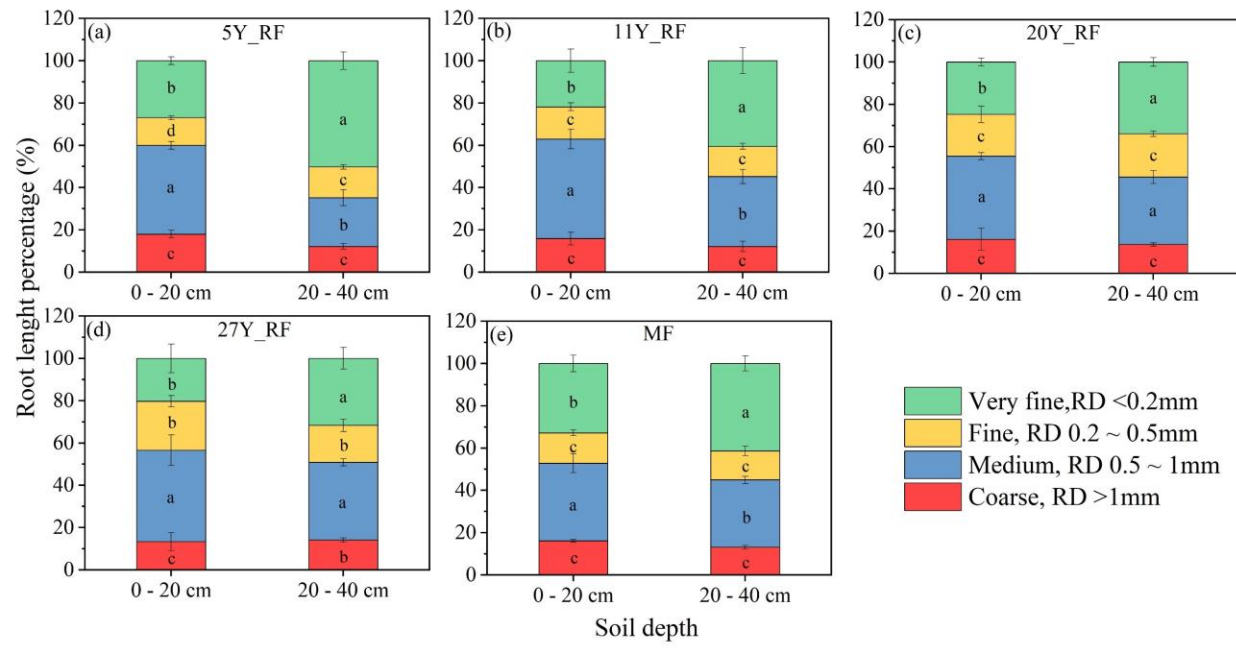
663 Note: BD: Bulk density; TOP: Total porosity; SMC: Soil moisture content; SOM: Soil organic matter; AN: Available nitrogen; AP:
664 Available phosphorus; AK: Available potassium.

665



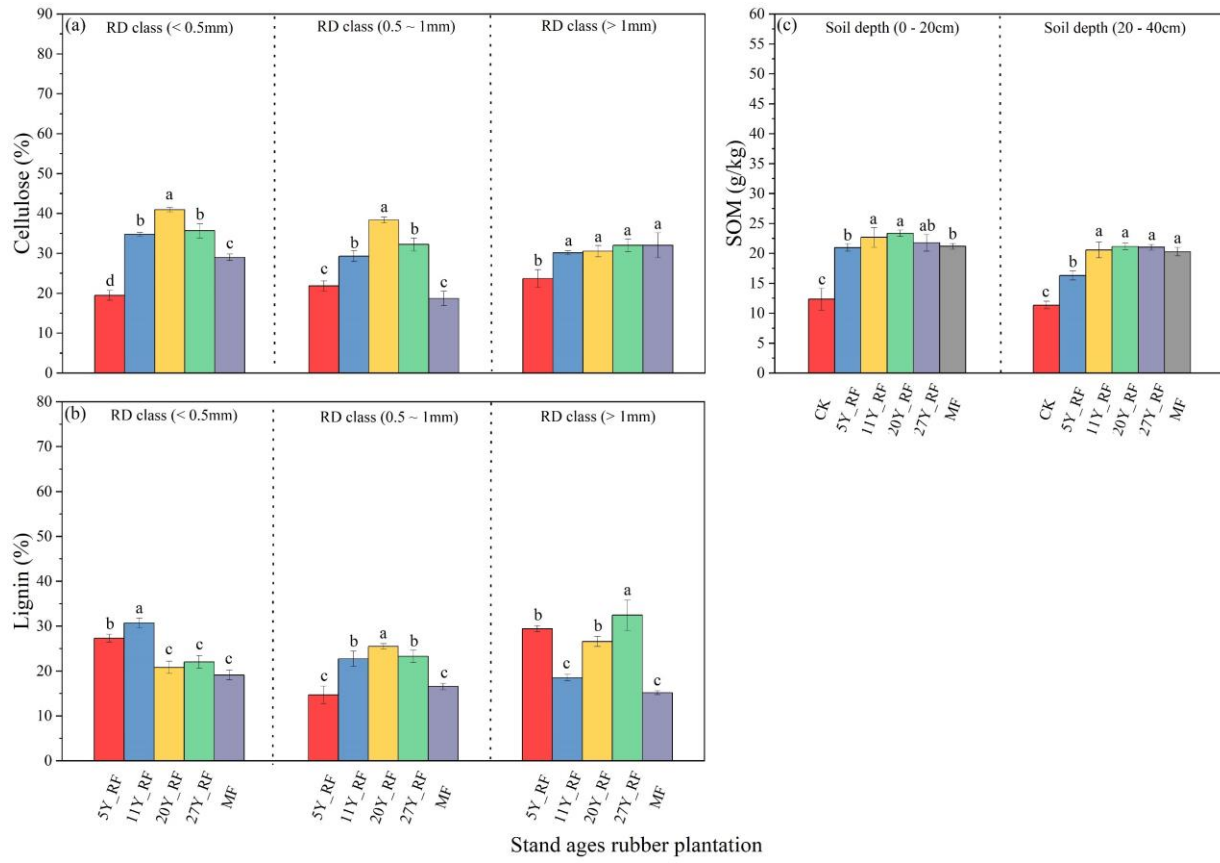
666

667 **Figure 1.** Different stand-age rubber plantation root morphological properties with soil depths.668 Each treatment was replicated three times (n = 3), and results are presented as mean \pm standard669 deviation. (a) Root diameter (RD), (b) Root length density (RLD), (c) Root surface area density670 (RSD), and (d) Root mass density (RMD).



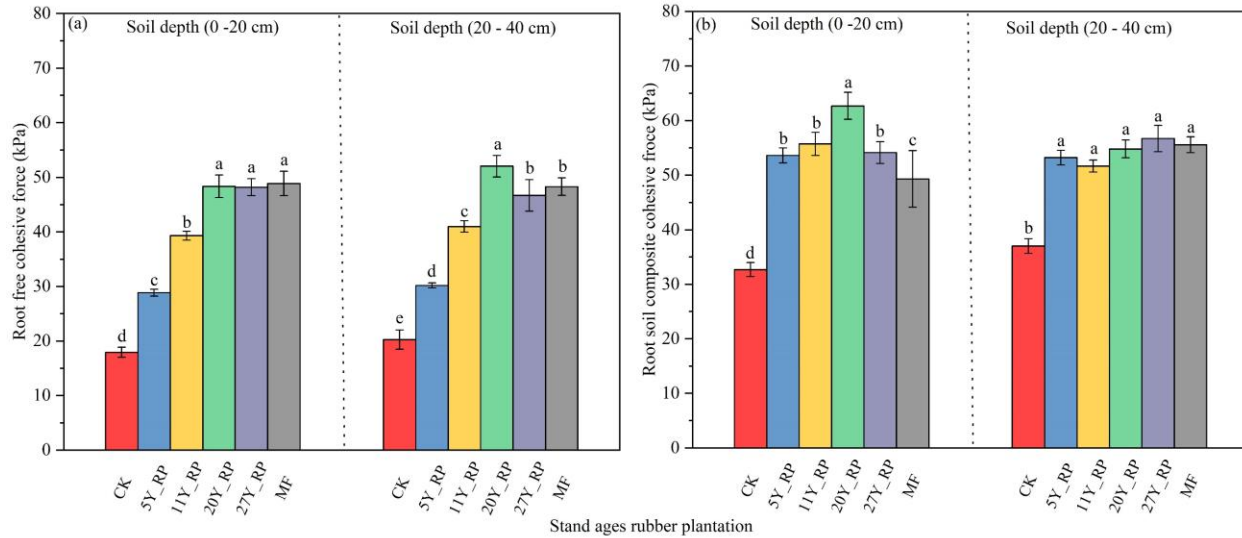
671

672 **Figure 2.** Root diameter distribution of rubber plants at different stand ages represented by the
 673 root length percentage across four class diameters. Each treatment was replicated three times (n =
 674 3), and results are presented as mean \pm standard deviation



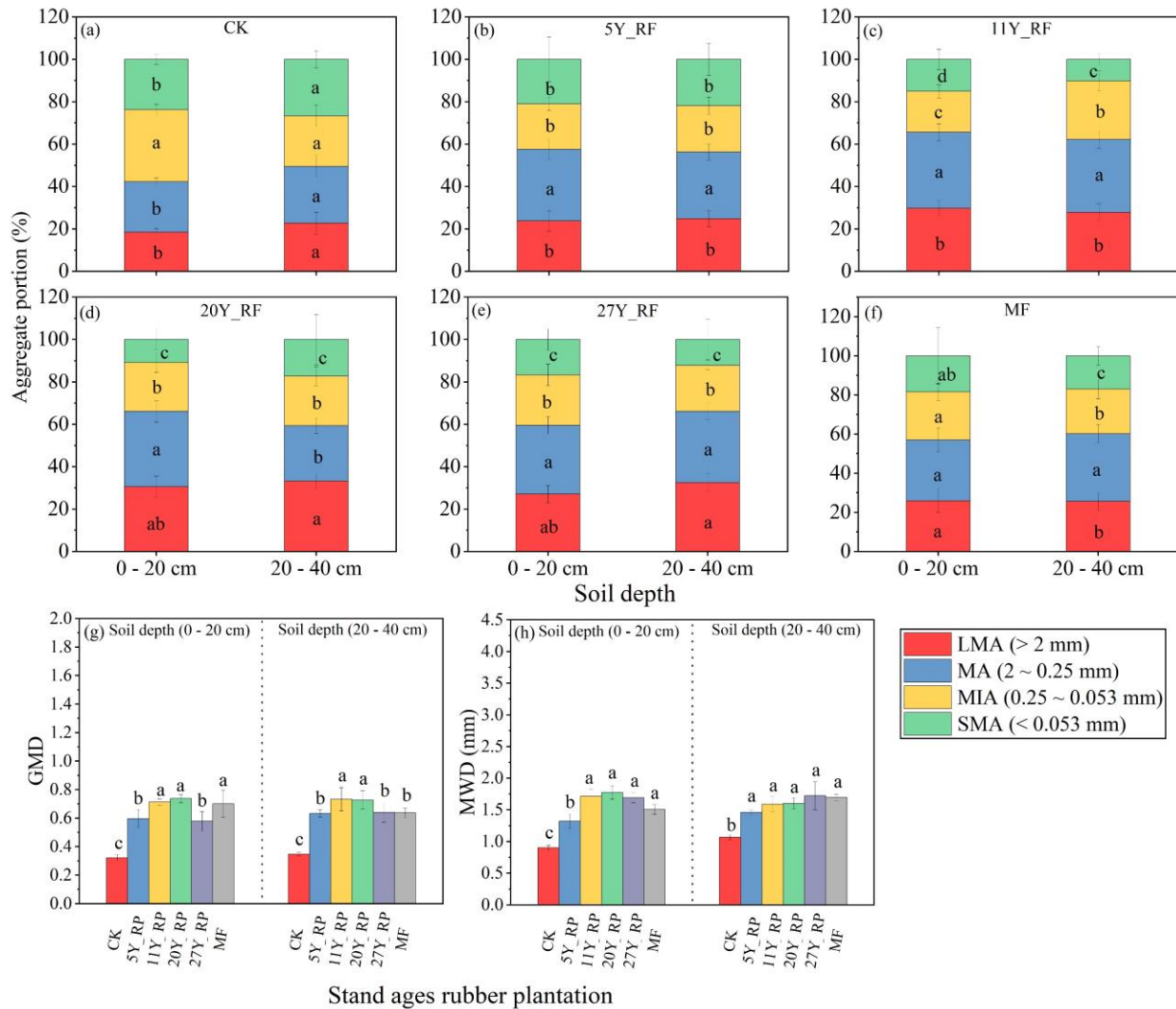
675

676 **Figure 3.** Different stand-age rubber plantation root chemical compositions and soil organic
 677 matter (SOM) distributions. Each treatment was replicated three times (n = 3), and results are
 678 presented as mean \pm standard deviation. (a) Cellulose, (b) Lignin, and (c) Soil organic matter
 679 (SOM).



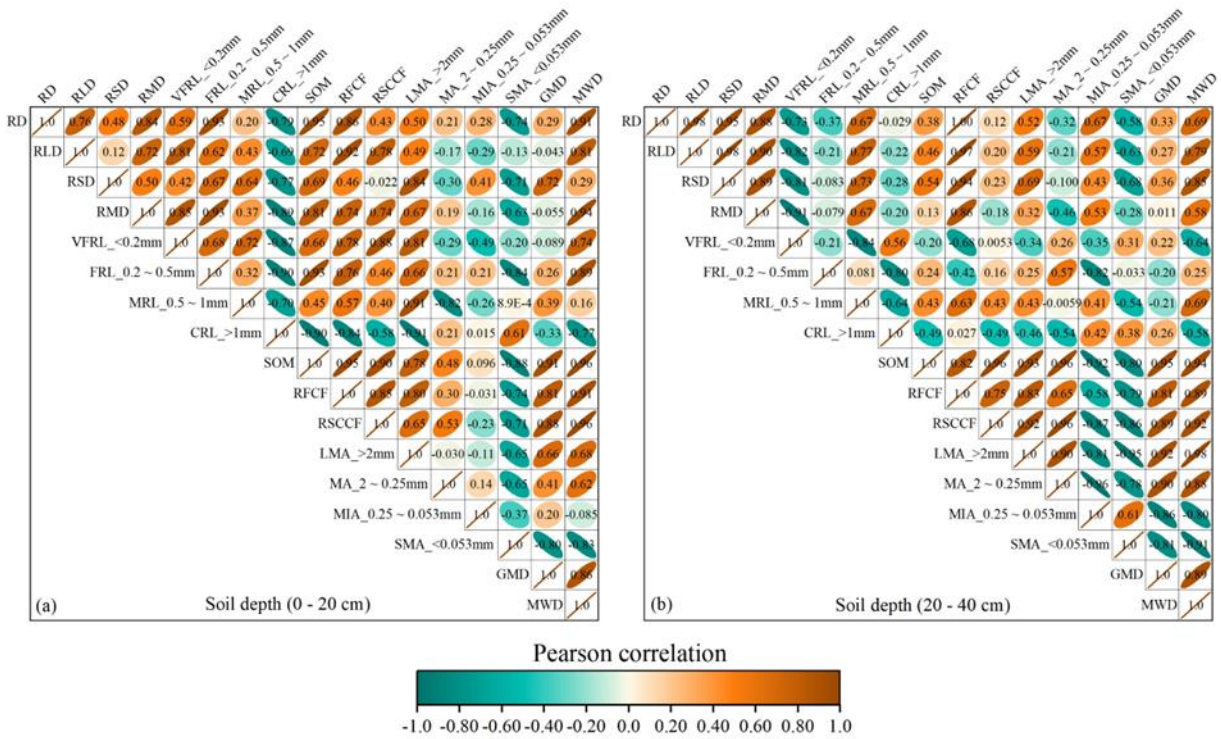
680

681 **Figure 4.** Soil cohesive force distribution under different stand-age rubber plantations. Each
 682 treatment was replicated three times (n = 3), and results are presented as mean \pm standard deviation
 683 (a) Root-free cohesive force (RFCS), (b) Root–soil composite cohesive force (RSCCF).



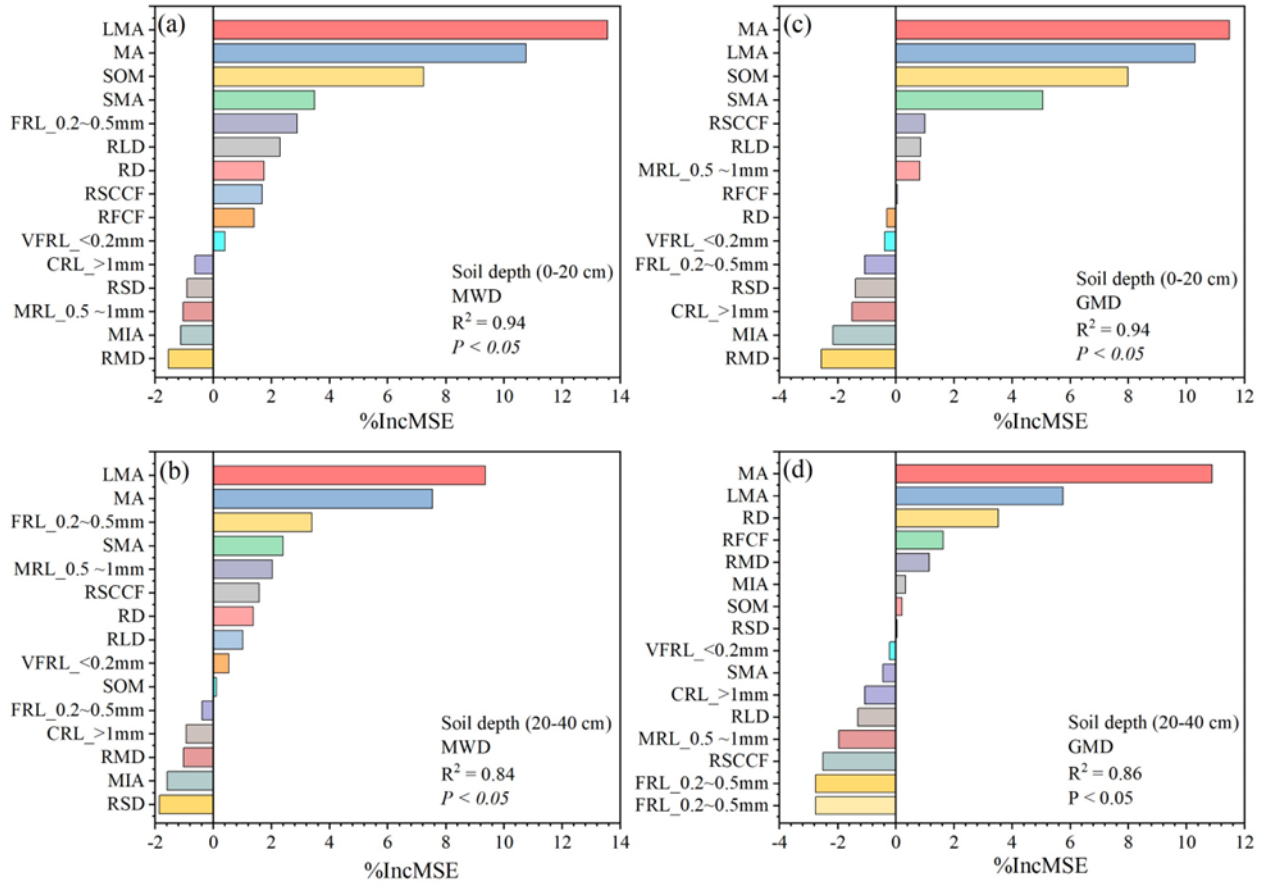
684

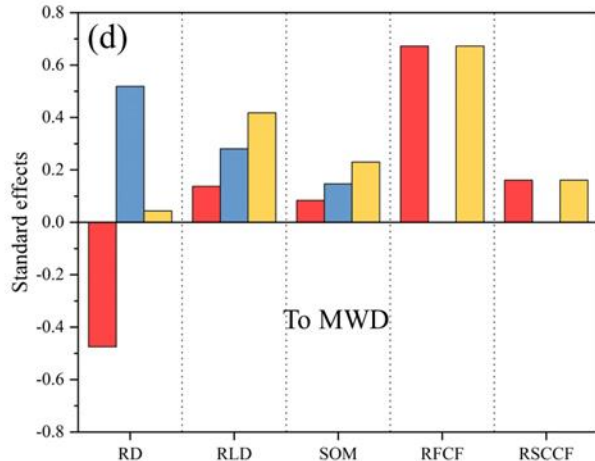
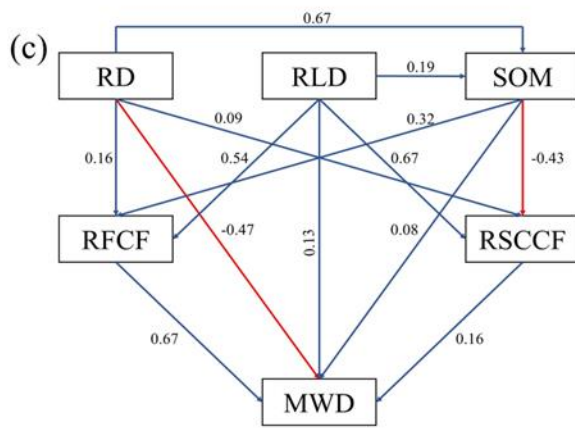
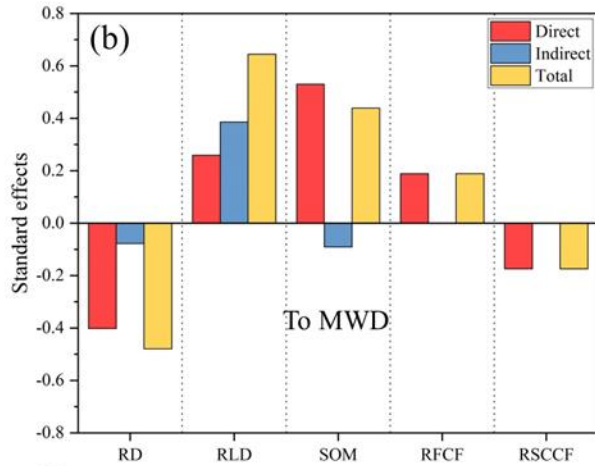
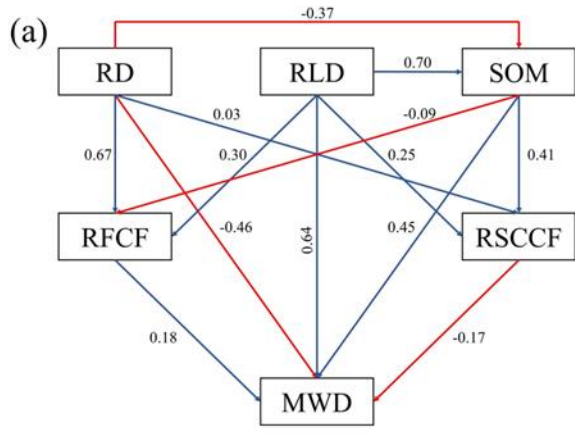
685 **Figure 5.** Different stand-age rubber plantation aggregate size distributions and soil aggregate
 686 stabilities (MWD and GWD) with soil depths. Each treatment was replicated three times (n = 3),
 687 and results are presented as mean \pm standard deviation.



688

689 **Figure 6.** Pearson correlations ($P < 0.05$) for all root traits, aggregate stabilities, soil organic
 690 matter, and soil cohesive forces. RD: root diameter; RLD: root length density; RSD: root surface
 691 area density; RMD: root mass density; VFRL: very fine root length; FRL: fine root length; MRL:
 692 medium root length; CRL: coarse root length; SOM: soil organic matter; RFCF: root-free cohesive
 693 force; RSCCF: root-soil composite cohesive force; LMA: large macroaggregates (> 2 mm); MA:
 694 macroaggregates (2–0.25 mm); MIA: microaggregates (0.25–0.053 mm); SMA: small
 695 microaggregates (< 0.053 mm); GMD: geometric mean diameter; MWD: mean weight diameter.
 696 The dark brown color indicates a positive correlation, and the pine green color indicates a negative
 697 correlation.





706

707 **Figure 8.** Partial least squares-path models (PLS-PM) ($P < 0.05$) indicating the indirect and direct
 708 impact of root properties, soil organic matter, and cohesive forces on soil aggregate stability at 0–
 709 20 cm (a, and b) and 20–40 cm (c, and d). The numbers near the arrows are standardized path
 710 coefficients. The blue line indicates the positive direction, and the red line indicates the negative
 711 direction. RD: root diameter; RLD: root length density; SOM: soil organic matter; RFCF: root-
 712 free cohesive force; RSCCF: root–soil composite cohesive force; MWD: mean weight diameter.